Journal of Magnetic Resonance 197 (2009) 71–76

Contents lists available at ScienceDirect

Journal of Magnetic Resonance

journal homepage: www.elsevier.com/locate/jmr

Direct measurements of protein backbone ^{15}N spin relaxation rates from peak line-width using a fully-relaxed Accordion 3D HNCO experiment

Kang Chen, Nico Tjandra *

Laboratory of Molecular Biophysics, National Heart, Lung, and Blood Institute, National Institutes of Health, 50 Center Drive, Bld. 50, Room 3513, Bethesda, MD 20892, USA

ARTICLE INFO

Article history:
Received 7 August 2008
Revised 14 November 2008
Available online 10 December 2008

Keywords:
Relaxation
HNCO
Accordion
Line width
Protein

ABSTRACT

Protein backbone ^{15}N spin relaxation rates measured by solution NMR provide useful dynamic information with a site-specific resolution. The conventional method is to record a series of 2D ^{1}H-^{15}N HSQC spectra with varied relaxation delays, and derive relaxation rate from the following curve fitting on the resonance intensities. Proteins with poorly resolved spectra often require several 3D HNCO spectra to be collected on a $^{15}N/^{13}C$ double labeled protein sample. In order to reduce the relaxation dimension Carr et al. (P.A. Carr, D.A. Fearing, A.G. Palmer, 3D accordion spectroscopy for measuring N-15 and (CO)-Carbon-13 relaxation rates in poorly resolved NMR spectra, J. Magn. Reson. 132 (1998) 25–33) employed an Accordion type HNCO pulse sequence to obtain ^{15}N or ^{13}C T_1 relaxation rates by numerical fitting of the relaxation interfered free induction decay (FID) data. To avoid intensive analysis of the time domain data, we propose a modified protocol to measure ^{15}N T_1 and T_2 relaxation rates from easily obtained line-widths in an Accordion HNCO spectrum. Both T_1 and T_2 relaxation could be simultaneously convoluted into the constant-time evolution periods of $^{13}C'$ and ^{15}N, respectively. The relaxation delay was allowed to reach at least $3 \times T_1$ or $3 \times T_2$ so that the signal was substantially decayed by the end of the FID, and the resulting peak full-width at half height (FWHH) could be directly used to calculate relaxation rate. When applied to the 76-residue Ubiquitin and the 226-residue glutamine-binding protein (GlnBP), this method yielded T_1 and T_2 values deviating on average by 4–6% and 5–7%, respectively, from the measurements based on the conventional 2D method. In comparison, the conventional methods possessed intrinsic error ranges of 2–4% for T_1 and 3–6% for T_2. In addition to comparable accuracy, the fully-relaxed Accordion HNCO method presented here allowed measurements of relaxation rates for resonances unresolved in 2D spectra, thus providing a more complete dynamic picture of the protein.

Published by Elsevier Inc.

1. Introduction

In solution NMR spectroscopy spin relaxation rates are linear summation of appropriate spectral densities derived from the rotational correlation function [1]. Knowledge of longitudinal (T_1) and transverse (T_2) relaxation rates provides rich dynamic information on the time scales ranging from sub-ns up to ms where conformational exchange contributes [2–4]. Generally for proteins, the dynamics studied with NMR can probe individual bond vectors connecting spin active nuclei. The most frequently measured spin nucleus is the ^{15}N backbone amide nitrogen, which reports on the dynamics of the N–H bond vector [5,6]. The conventional way to measure ^{15}N spin relaxation rates (T_1 or T_2) is to record a series of 2D ^{1}H-^{15}N HSQC spectra with various relaxation delays. The corresponding peak intensities are fit with an exponential decay function to obtain the relaxation rates. For proteins with poorly resolved ^{1}H-^{15}N spectra, several 3D HNCO spectra with varied relaxation delays, which correlate the $^{1}H_i$-$^{15}N_i$ moiety to spin of carbonyl $^{13}C'_{i-1}$ in the third dimension, can be collected instead [7,8]. This solves the peak-overlap problem at the cost of experimental time.

One approach to shorten experimental time is to reduce dimensionality. Since both the spin relaxation scheme and the heteronuclear (^{15}N or ^{13}C) evolution period in triple-resonance pulse sequences are time dependent functions, it is possible to convolute the two. The idea of mixed-evolution was originally applied in measuring chemical exchange rates, and the type of pulse sequence was referred to as Accordion experiment because the time coordinate of the exchange was stretched or squeezed because of mixing, by Bodenhausen and Ernst [9,10]. Later Kay and Prestegard estimated proton T_1 from the null position along the indirect t_1 evolution profile using an Accordion type COSY pulse [11]. Mandel and Palmer and Carr et. al. first employed the Accordion method to project T_1 relaxation of ^{15}N or $^{13}C'$ onto the t_1 evolution period of the like nucleus in a constant-time version of 3D HNCO experiment [12,13]. In their method the full t_1 evolution profile, or free induction decay (FID), is obtained in two parts, termed as a "negative

* Corresponding author. Fax: +1 301 402 3405.
E-mail address: tjandran@nhlbi.nih.gov (N. Tjandra).

1090-7807/$ - see front matter Published by Elsevier Inc.
doi:10.1016/j.jmr.2008.12.001

time" manner, to minimize any transverse relaxation leakage during t_1. The subsequent minimization of t_1 interferogram yields spin relaxation rates and Larmor frequencies, using the hankel singular value decomposition (HSVD) algorithm [14] and Levenberg–Marquardt nonlinear least-square fitting routine.

We are proposing a fully-relaxed type of Accordion HNCO experiment to measure ^{15}N relaxation rates, aiming to ease both acquisition and computational work. Both T_1 and T_2 relaxation processes were synchronized with heteronuclear evolution periods. The relaxation delay period covered at least $3 \times T_1$ or $3 \times T_2$ so that the full-relaxation should be ensured for nearly every nucleus. The spin relaxations time constants were directly estimated from peak full-width at half height (FWHH) on the corresponding indirect dimensions. Our protocol yielded comparable accuracy of relaxation rates as the conventional method for the model proteins 76-residue Ubiquitin and 226-residue glutamine-binding protein (GlnBP). In addition, for the medium sized protein GlnBP, which consists of similar contents of α-helix and β-sheet [15], the proposed method allowed measurements for 97% of assigned spin nuclei, in contrast to the 79% from the typical 2D method. The improvement is expected to be even more dramatic for α-helix rich proteins and unfolded proteins with less-dispersive resonances.

2. Materials and methods

2.1. Pulse sequence and acquisition parameters

The published gradient-enhanced sensitivity HNCO pulse sequence [16] was adopted with the addition of backbone ^{15}N relaxation blocks and the adjustment for constant-time evolutions (Fig. 1A). The magnetization transfer will not be repeated here, but specifically the in-phase N_x magnetization was prepared right before the T_2 relaxation loop, subject to the later transverse and longitudinal spin relaxation. Since the relaxation delay increment was synchronized with heteronuclear evolution, the envelope of the FID in the indirect dimension should code solely for the relaxation incorporated exponential decay function with the use of constant-time acquisition. The pulse sequence was tested using 1 mM ^{15}N/^{13}C doubly labeled Ubiquitin and GlnBP samples on a 600 MHz Bruker DMX spectrometer equipped with a triple-resonance TXI probe containing an *xyz*-gradient coil. Most pulse sequence related acquisition parameters were described in the caption of Fig. 1.

For Ubiquitin the temperature was set at 293 K. The carrier frequencies were set at 4.80 ppm for ^{1}H, 115.4 ppm for ^{15}N, 178.1 ppm for ^{13}C′, and 56.1 ppm for ^{13}C$^{\alpha}$. The spectral widths were set as 7184 Hz for ^{1}H, 1786 Hz for ^{15}N, and 1563 Hz for ^{13}C′. The number of real data points collected on ^{1}H, ^{15}N and ^{13}C′ dimensions were 512, 41 (*Npts*) and 51 (*Cpts*), respectively. During acquisition the loop counters for T_2 and T_1 relaxation (Fig. 1B) were incremented from 0 to *Npts*-1 and *Cpts*-1, respectively. It is essential to let the last relaxation delay reach a period longer than $3 \times T_1$ or $3 \times T_2$, to avoid truncation effects during FT. T_2 and T_1 relaxation unitary blocks were 12 and 32 ms in length, respectively (Fig. 1B), thus the intensities of the last collected points on ^{15}N and ^{13}C′ FIDs code for relaxation delays of 480 ms (40×12 ms) and 1600 ms (50×32 ms), respectively. The total experimental time for T_1 and T_2 incorporated fully-relaxed type of Accordion HNCO experiment was 79 h with 1.1 s recycle delay, 16 scans per FID, and 512 dummy scans.

For GlnBP the temperature was set at 312 K. The carrier frequencies were set at 4.61 ppm for ^{1}H, 117.9 ppm for ^{15}N, 176.0 ppm for ^{13}C′, and 56.1 ppm for ^{13}C$^{\alpha}$. The spectral widths used were 7184 Hz for ^{1}H, 2174 Hz for ^{15}N, and 1667 Hz for ^{13}C′. T_2 and T_1 relaxations were collected separately using two HNCO experiments because of low sensitivity associated with dual-collection within one experiment. Both relaxation schemes were convoluted with ^{15}N evolution. For the T_1 encoded HNCO experiment the number of real data points collected on ^{1}H, ^{15}N and ^{13}C′ dimensions were 512, 41 (*Npts*) and 39 (*Cpts*), respectively. For the T_2 encoded HNCO experiment the number of real data points collected on ^{1}H, ^{15}N and ^{13}C′ dimensions were 512, 43 (*Npts*) and 48 (*Cpts*), respectively. Different from the set-up for Ubiquitin, the numbers of 180° pulses in Fig. 1B were adjusted so that T_2 and T_1 relaxation unitary blocks were 6 and 64 ms in length, respectively. The total experimental time for T_1 and T_2 separately incorporated fully-relaxed type of Accordion HNCO experiment were 79 and 63 h, respectively, with 1.1 s recycle delay, 16 scans per FID, and 512 dummy scans.

2.2. Data processing and extraction of T_1 and T_2

Generally, every FID from direct dimension (^{1}H) was apodized with a cosine function and zero-filled to double the number of data points. FIDs in the ^{15}N and ^{13}C′ dimensions were either apodized with a cosine function or left untouched if relaxation parameters were going to be extracted from this dimension. Nevertheless, FIDs on all indirect dimensions were zero-filled to 512 points before FT and no phase correction was applied. The first data point on each FID, both direct and indirect, was scaled by half before FT. The final 3D spectra were generally stored in a matrix size of $400(^1\text{H}) \times 512(^{15}\text{N}) \times 512(^{13}\text{C}')$.

Relaxation parameters T_1 and T_2 were always extracted separately from differently processed spectra even if both could be collected within the same HNCO experiment. For instance, for Ubiquitin when T_1 was going to be extracted according to natural line-width in the ^{13}C′ dimension, apodization was applied to the ^{15}N dimension which encoded the T_2 relaxation to give a better resolution, and *vice versa*.

In theory Fourier transform of a sinusoid curve convoluted with a single exponential decay function should yield a Lorentzian-shaped peak with its FWHH corresponding to the inverse of decay time constant (T) (Eq. (1)). However, in the Accordion experiment the time axis labeling for chemical shift evolution is different from that for relaxation delay. The time scaling factor κ, in the same definition as Carr et al. [12] is needed to account for the difference. In Eq. (2) T_B was the time period of one unitary block for the T_1 or T_2 loop (Fig. 1B) and Δt, the inverse of spectral width, was the time evolution between two successive real points in indirect dimension; the difference of the two defined the Accordion type stretching or squeezing of the time axis. The measured FWHH, could then be converted to a real relaxation time constant T using Eq. (3).

$$\text{FWHH} = 1/(\pi T) \tag{1}$$

$$\kappa = T_B/\Delta t \tag{2}$$

$$T = \kappa/(\pi \times \text{FWHH}) \tag{3}$$

2.3. Correction to T_1 and T_2

Relaxation time constants for most amide ^{15}N nuclei were measured with the protocol described above. However, because of truncation effects during FT, extremely long relaxation time constants could be under-estimated. Application of an exponential decay or line-broadening function before FT was adopted to obtain long T_1 and T_2. A simple slope check procedure was performed to identify spins requiring forced-damping on the FID. Basically, data processing was repeated three times with the only difference being the line-broadening (*lb*) function applied to the target domain with the size of 0, 0.5 *c*, and *c* Hz for *lb*, which yielded three relaxation time constants T for each spin nucleus using Eq. (4). The slope of

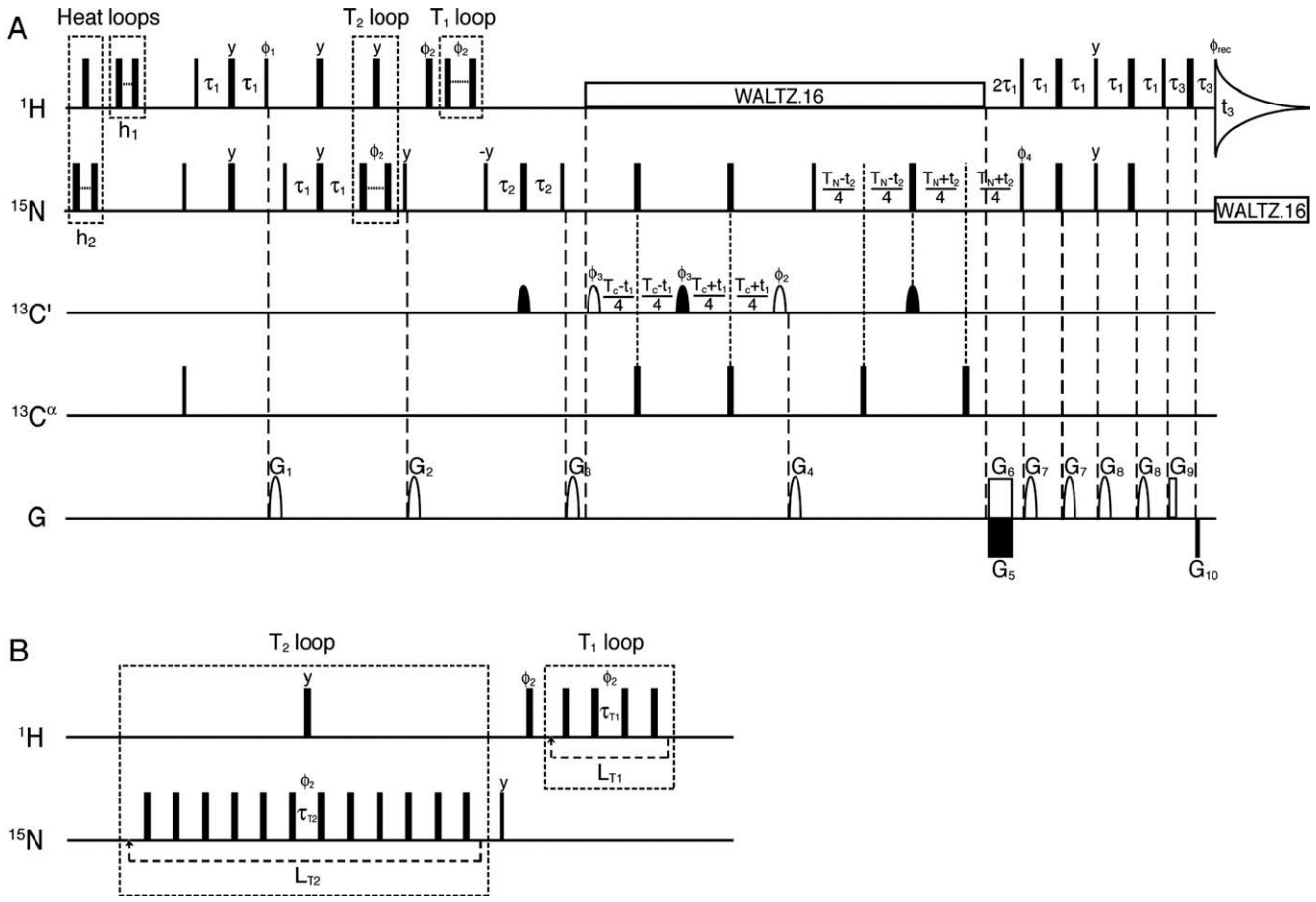

Fig. 1. The 3D fully-relaxed type of Accordion HNCO pulse sequence for measuring ^{15}N spin relaxation rates (A) with enlarged details for T_1 and T_2 blocks (B). Narrow and wide rectangular pulses correspond to flip angle of 90° and 180°, respectively. Open and filled shaped pulses on carbonyl ^{13}C′ channel are sinc-shaped 90° and 180°, respectively. The ^{1}H and ^{15}N Waltz decoupling pulse strength was 4.2 kHz and 1.3 kHz, respectively. The RF used for carbonyl ^{13}C′ pulse was 1.3 kHz. The ^{13}C$^{\alpha}$ pulse width was 53 and 47.4 μs for flip angle of 90° and 180°, respectively. The default pulse phase is along x. Phase cycles are listed as follows, $\varphi_1 = y, -y$; $\varphi_2 = (x)_4, (-x)_4$; $\varphi_3 = (x)_2, (-x)_2$; $\varphi_4 = -x$; $\varphi_{rec} = x, (-x)_2, x, -x, (x)_2, -x$. Delay durations τ_1, τ_2, and τ_3, are 2.6, 12.5, and 0.25 ms, respectively. The duration, strengths and direction for gradient pulses were as follows, G_1 = 1.1 ms, 12.5 G/cm, y; G_2 = 1.0 ms, 10 G/cm, x; G_3 = 0.7 ms, 12.5 G/cm, y/z; G_4 = 1.3 ms, 17 G/cm, y; G_5 = 2.694 ms, −17 G/cm, z; G_6 = 2.694 ms, 17 G/cm, z; G_7 = 1.0 ms, 17 G/cm, x; G_8 = 1.0 ms, 17 G/cm, y; G_9 = 0.2 ms, 17 G/cm, z; G_{10} = 0.0756 ms, −30 G/cm, z. Gradient pulses G_5, G_6, G_9, and G_{10} were rectangular shaped while the rest were sine-shaped. Quadrature detection on the ^{15}N dimension was achieved via Echo–Antiecho method [23–25]. P- and N-type coherences were collected for each increment of t_2 with the gradient pulse switch between G_5 and G_6. Concomitantly ^{15}N pulse phase φ_4 had to be interchanged between $-x$ and $+x$ for P- and N-coherence selection. Quadrature detection on ^{13}C′ dimension was achieved via States-TPPI method [26] by incrementing ^{13}C′ pulse phase φ_3 and receiver phase φ_{rec}. The constant-time period for ^{15}N evolution (T_N/4) needs to be the larger value of 5.5 ms and ($Npts$+1) × (Δt_N/4), where $Npts$ is the total real points on ^{15}N dimension and Δt_N equals the inverse of ^{15}N spectral width. Similarly the constant-time period for ^{13}C′ evolution (T_C/4) equals ($Cpts$+1) × (Δt_C/4), where $Cpts$ is the total real points on ^{13}C′ dimension and Δt_C is the inverse of ^{13}C′ spectral width. The 180° pulse repetition delays τ_{T1} and τ_{T2} in T_1 and T_2 blocks was set as 8 and 1 ms, respectively, but they could be customized. The loop counters L_{T1} and L_{T2}, initialized as 0, had to be co-incremented with either ^{15}N or ^{13}C′ evolution. L_{T1} and L_{T2} ranged from 0 to $Cpts$-1 and $Npts$-1, respectively, during acquisition. The beginning blocks for heat compensation should be identical to T_1 and T_2 blocks except that τ_{T1} might be shortened to 0.2 ms. The loop counters h_1 and h_2 were decremented from the initial values of $Cpts$ and $Npts$, respectively, to 1, in concert with the incrementing of L_{T1} and L_{T2} so that the total number of ^{1}H and ^{15}N pulses stayed the same from scan to scan.

T vs. lb for each nucleus was obtained using linear regression. The average slope $\langle s \rangle$ and its standard deviation SD were calculated. Slopes above $\langle s \rangle$ + 1.5 SD were considered to indicate underestimation of T_1 or T_2.

$$T = \kappa/[\pi(\mathrm{FWHH} - lb)] \quad (4)$$

$$LW_N = 4/[\pi(Npts - 1)\Delta t_N] \quad (5)$$

The size of c was chosen based on the criterion that the average peak FWHH, for instance, in the ^{15}N dimension, from the spectrum processed with a line-broadening of c Hz would be close to the target line-width LW_N specified in Eq. (5), where Δt_N was the inverse of spectral width on the ^{15}N dimension. The value of LW_N was expected to be the lower limit for the obtainable line-width free of truncation effects, which required a smooth decay of ^{15}N FID signal to noise level or null. Following the above reasoning, the denominator $(Npts - 1)\Delta t_N$ in Eq. (5), the full evolution time for ^{15}N spin nuclei, should cover the length of several (>3) apparent exponential time decay constants of the FID curve. For simplicity a value of 4, the numerator in Eq. (5), was used, and the magnitude of the last point on the apodized FID was expected to be about 1.8% (e^{-4}) of the initial intensity. Ideally the numerator in Eq. (5) should equal ln(S/N) for individual spin, however, a global value is chosen here as a good compromise for the purpose of checking for the slope. The target line-width LW_C for ^{13}C′ dimension could be calculated similarly using Eq. (5).

Not all spins identified with significantly high slope (T vs. lb) were subject to the correction. The second filter was their S/N ratio. Spins with their S/N larger than the sum of mean and standard deviation, calculated from the first spectrum (lb = 0 Hz) of the above three, were chosen for correction. The correction was performed for each spin nucleus that required it. That is, one line-broadening processing was performed specifically for one spin. The corrected relaxation time constant was calculated using Eq. (4). The size of lb was chosen so that the resulted FWHH for that

spin reached the mean value of line-width from the first spectrum that carried 0 Hz line-broadening during processing.

2.4. Conventional method for T_1 and T_2

The reference T_1 and T_2 values were measured using conventional 2D method [17]. Identical relaxation blocks (Fig. 1B) were kept in the corresponding HSQC pulses. Six spectra were collected for each measurement with varied relaxation delay covering the range of 0–1.5 T_1 or 1.5 T_2. The standard deviation from the curve fitting was used as the intrinsic error range of the measurement. For accuracy comparison with the fully-relaxed Accordion method, the pair-wise difference, $|T_{\text{accord.}} - T_{\text{conv.}}|/T_{\text{conv.}}$, was calculated for each spin resolvable in the 2D spectra and the average of differences was presented.

The program NMRPipe was employed for all NMR data processing [18]. The measurement of FWHH and exponential curve fitting were carried out using the routines in Sparky 3.1. (T.D. Goddard and D.G. Kneller, UCSF) The linear regression was performed in Grace 5.1. (Grace Development Team).

3. Results

Generally when tested on Ubiquitin and GlnBP, the proposed NMR data processing protocol yielded satisfactory sensitivity and resolution of the HNCO spectrum. Most of the relaxation time constants were measured from FWHH on the spectrum that had no line-broadening function applied (*lb* = 0 Hz). A couple of spins with sufficient *S/N* ratio were subject to specific correction. Some important acquisition and processing parameters were presented in Table 1. Complete results on the two proteins were as follows.

3.1. Ubiquitin

The backbone chemical shift assignments of Ubiquitin were taken from Wang et al. [19]. A total of 70 peaks out of 76 residues were observed on the current Accordion type HNCO spectrum with the absence of M1, P19, P37, P38, E24, and G53, the last two of which experience significant conformational exchange [20]. ^{15}N T_2 and T_1 relaxations were synchronized with ^{15}N and ^{13}C′ evolutions, respectively. Typical relaxation incorporated FIDs on ^{13}C′ and ^{15}N dimensions were shown in Fig. 2A and B, respectively, for residue I13. FT of indirect FIDs without any apodization should yield T_1 and T_2 from FWHH (Fig. 2C) with proper conversion using Eq. (3). Although it was possible to measure T_1 and T_2 simultaneously from one spectrum as shown in Fig. 2C, we realized better sensitivity and resolution could be obtained if T_1 and T_2 were extracted separately from individually processed spectra.

We extracted the T_2 employing the described protocol. First the raw NMR data were processed with zero line-broadening applied (*lb* = 0 Hz) on the ^{15}N time domain and a cosine apodization on the ^{13}C′ dimension. The line-width, FWHH, was measured for all spins and T_2 was calculated using Eq. (3). We had to decide if correction was needed for some long T_2 nuclei. The average FWHH of the resonances along the ^{15}N dimension was 48.5 Hz (*lb* = 0 Hz), away from the target value LW_N of 56.8 Hz. When line-broadening of 10 Hz, the value of *c*, was applied during processing, the average FWHH became 56.5 Hz, matching the target value LW_N. A triple processing of the raw data with *lb* value of 0, 5 and 10 Hz was performed and T_2 out of each processing were calculated using Eq. (4). The following linear regression on T_2 vs. *lb* curve could reveal spins that have extremely long T_2. Shown in Fig. 3 were typical slope check results for the spin with regular T_2, ^{15}N of residue I13 yielding flat slope, and the one with extremely long T_2, ^{15}N of residue G76 yielding significantly positive slope. ^{15}N spins of residues R74 through G76 were identified to have significant positive slope (>mean + 1.5 SD). Since the line-broadening correction would reduce *S/N* ratio and affect accuracy of extracted FWHH, only spins with sufficient *S/N* ratio to start with were chosen. All identified three residues R74-G76 had enough *S/N* ratio according to the

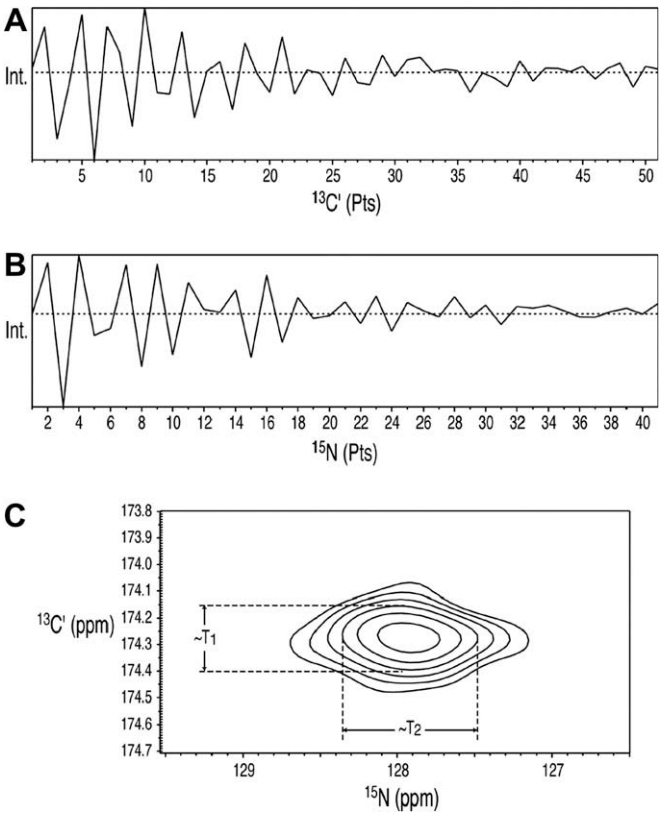

Fig. 2. Examples of relaxation incorporated FIDs on indirect dimensions (A, B) and their Fourier transformed spectrum (C). Traces of FIDs for residue I13 of Ubiquitin were shown along T_1 convoluted ^{13}C′ dimension (A) and T_2 convoluted ^{15}N dimension (B). The dashed line indicated the zero intensity (A and B). T_1 or T_2 could be estimated from line-width on the corresponding dimension (C).

Table 1
Essential acquisition, processing parameters, and results of fully-relaxed Accordion HNCO experiment.

Protein		Dimension[a]	*Npts*/*Cpts*	$\Delta t_N/\Delta t_C$ (μs)	T_B (ms)	*c* (Hz)	Average FWHH (Hz)	LW_N/LW_C (Hz)	Pair-wise difference (%)[b]	Intrinsic error range (%)[c]
Ubi	T_1	13C′	51	640	32	8	32.8	39.8	3.6	1.5
	T_2	^{15}N	41	560	12	10	48.5	56.8	4.7	2.9
GlnBP	T_1	^{15}N	41	460	64	18	55.0	69.2	5.6	3.8
	T_2	^{15}N	43	460	6	7	59.8	65.9	7.4	6.4

[a] The evolution period of nucleus where relaxation was incorporated.
[b] For Ubiquitin all available measurements, spins from 70 residues, from both methods were compared. For GlnBP only 176 measurements from the conventional 2D methods were available for comparison.
[c] The average standard deviations out of curve fitting in the conventional method were treated as the error range.

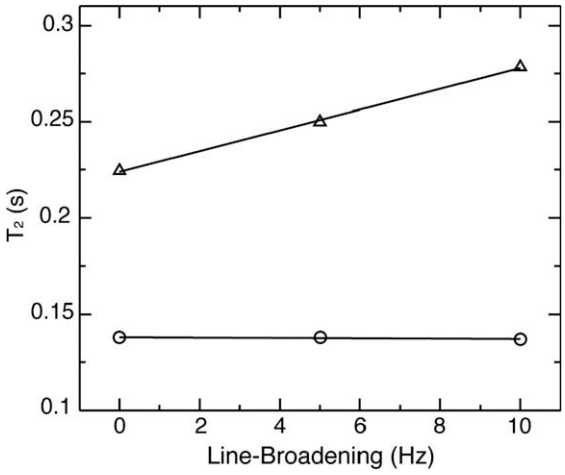

Fig. 3. Plot of typical T_2 vs. *lb* slopes, flat or steep. Residues I13 and G76 of Ubiquitin were shown in circles and triangles, respectively. T_2 of residue G76 was underestimated and required line-broadening correction.

criterion stated in Section 2. The correction value of *lb* was chosen for each spin to ensure the resulted ^{15}N FWHH of that spin roughly equal, within 1 Hz difference, the mean FWHH value from the first processed spectrum with no line-broadening applied. The values of *lb* were 22, 29 and 32 Hz for residues R74, G75 and G76, which also indicated the increasing T_2 values towards the C-terminus of Ubiquitin. The final T_2 values for all 70 spins differ on average by 4.7% from those measured using conventional 2D methods. The pairwise difference is comparable to the intrinsic uncertainty, 2.9%, associated with conventional 2D methods.

A similar treatment was used to extract T_1 values from the $^{13}C'$ dimension. Corrections were made on the spins of residues G75 and G76. The final T_1 values differ on average by 3.6% from those measured using conventional 2D methods, while the latter possesses an intrinsic uncertainty of 1.5%.

The comparison of T_1 and T_2 profiles between the fully-relaxed Accordion method and the conventional method are shown in Fig. 4. Some essential acquisition and processing parameters are presented in Table 1.

3.2. Glutamine-binding protein

We also tested our method on the 226-residue glutamine-binding protein. The backbone spin assignments of GlnBP, missing

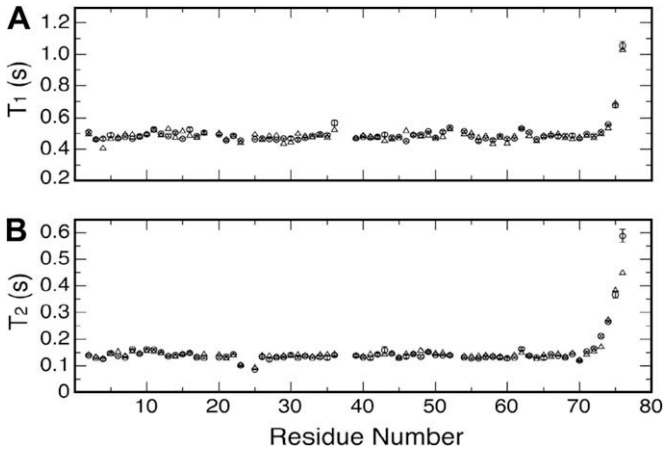

Fig. 4. Comparisons of T_1 (A) and T_2 (B) profiles of Ubiquitin measured using the fully-relaxed Accordion 3D HNCO method (triangle) and the conventional 2D method (circles). Error bars for conventional method were standard deviations out of curve fitting.

HNCO correlations for residues A1, D2, P15, P47, P55, P137, P159, P190, P225, G21, D22, D73, and N97-99, were taken from Yu et al. [21]. We further excluded non-observed residues K131 and G171 and overlapping residues L146, K205, F81, and F189. A total of 205 peaks remained for analysis. For relatively large proteins like GlnBP short $^{13}C'$ T_2 will result in relatively low sensitivity and the longer ^{15}N T_1 will increase experimental time in the T_1 and T_2 doubly coded Accordion HNCO experiment. We chose to incorporate T_1 and T_2 relaxations separately into two HNCO experiments, and both were encoded on the ^{15}N dimension thus leaving $^{13}C'$ dimension solely for peak-resolving purposes.

Similar data processing to Ubiquitin was applied. Essential acquisition and processing parameters are shown in Table 1. Almost all relaxation time constants were measured without applying any line-broadening. Corrections were made for T_2 of residue K226 and T_1 of residue K37. The final T_2 and T_1 values differ on average by 7.4% and 5.6%, respectively, from those measured using conventional 2D methods, while the latter possesses an intrinsic uncertainty of 6.4% and 3.8% for T_2 and T_1, respectively. It is worth noting relaxation times for only 167 residues were available from the 2D method and used for the pair-wise comparison, while those from 205 residues were measured using the fully-relaxed Accordion method (Fig. 5).

4. Conclusions and discussions

We demonstrated the applicability of using a fully-relaxed Accordion type 3D HNCO pulse sequence to measure T_1 and T_2 values from peak line-width. Both relaxations could be measured within one HNCO experiment, given sufficient sensitivity. The current method to extract T_1 and T_2 values are different from the original Accordion approach [12], which includes numerical minimization on indirect FIDs. The sensitivity can be further improved by the availability of the cryogenic probe and sample perdeuteration. Though the gradient-enhanced version of HNCO pulse sequence was adopted here, the TROSY-HNCO pulse scheme can be easily adapted to help the sensitivity issue associated with larger proteins.

The major consideration during acquisition was that the final relaxation delay should reach $3 \times T_1$ or $3 \times T_2$ so that the peak line-width is relatively insensitive to truncation effects during FT. The data processing is largely straightforward. The accuracy is comparable to conventional 2D methods. In addition, for the 226-residue protein GlnBP, which possesses appreciable amount of β-sheet structure, we obtained relaxation data for over 23% more spin nuclei than those from the 2D method. The improvement is expected to be more significant for α-helix rich proteins that typically have worse resonance dispersion in 2D ^{1}H-^{15}N HSQC spectra. One may also measure relaxation times using conventional method with several 3D HNCO spectra [7,8] being collected at optimal relaxation delay intervals of $0–1.2 \times T$ [22]. The total Accordion HNCO acquisition time is 63 h for the T_2 measurement of GlnBP. The time period for an HNCO experiment with the same set-up is about 36 h. Thus the conventional discrete sampling method using HNCO pulses and the same amount of spectrometer time will allow 2-point or alternatively 4-point collection can be achieved if the number of real points in ^{13}C dimension is cut in half. However, a Monte–Carlo simulation shows more accurate measurements with error range of about 4% can be obtained with Accordion method, while about 7% error will be in the 2-point or 4-point sampling (Supplementary material). This is primarily due to the Accordion method sampling more points, equal to the number of indirect FIDs, on the relaxation decay curve.

In addition to T_1 and T_2 the heteronuclear ^{1}H-^{15}N NOE data are necessary to provide complementary dynamics on sub-ns time

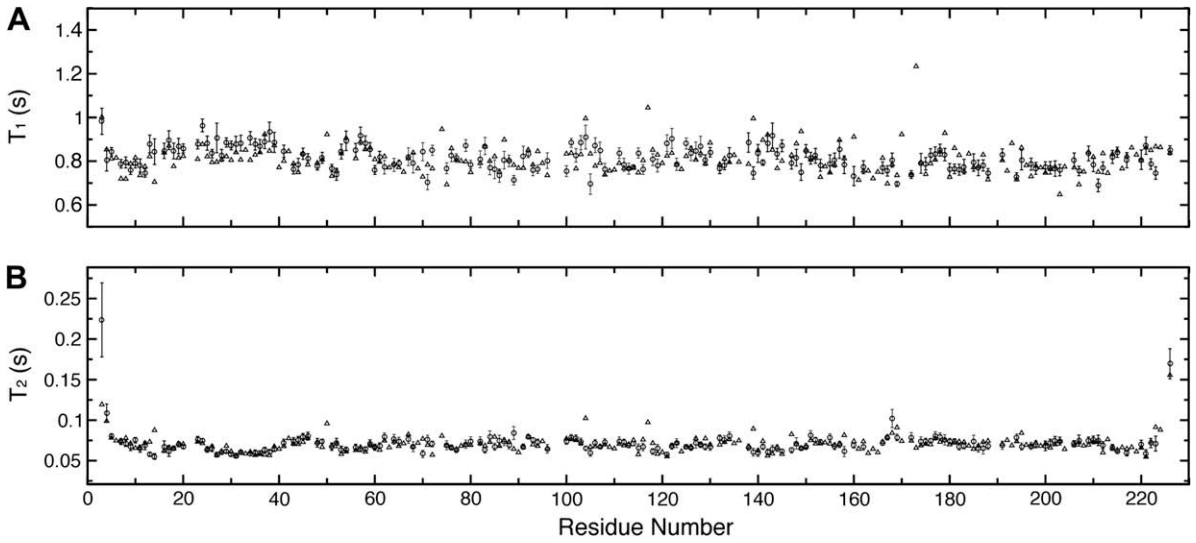

Fig. 5. Comparisons of T_1 (A) and T_2 (B) profiles of GlnBP measured using the fully-relaxed Accordion 3D HNCO method (triangle) and the conventional 2D method (circles). Error bars for conventional method were standard deviations out of curve fitting.

scale. This experiment only requires two measurement points and the HNCO version for NOE measurements are available elsewhere [7,8]. The presented fully-relaxed Accordion experiment, maximally exploiting the advantage of resolution from heteronuclear NMR, should offer a more complete and site-specific picture of dynamics of potentially challenging proteins.

Acknowledgments

We thank James Gruschus for careful reading of the manuscript. This work was supported by the Intramural Research Program of the NIH, National Heart, Lung, and Blood Institute.

Appendix A. Supplementary data

Supplementary data associated with this article can be found, in the online version, at doi:10.1016/j.jmr.2008.12.001.

References

[1] J. McConnell, The Theory of Nuclear Magnetic Relaxation in Liquids, Cambridge University Press, Cambridge, New York, 1987.
[2] G.M. Clore, P.C. Driscoll, P.T. Wingfield, A.M. Gronenborn, Analysis of the backbone dynamics of interleukin-1-beta using 2-dimensional inverse detected heteronuclear N-15-H-1 NMR-spectroscopy, Biochemistry 29 (1990) 7387–7401.
[3] A.G. Palmer, Probing molecular motion by NMR, Curr. Opin. Struc. Biol. 7 (1997) 732–737.
[4] A.G. Palmer, C.D. Kroenke, J.P. Loria, Nuclear magnetic resonance methods for quantifying microsecond-to-millisecond motions in biological macromolecules, Method. Enzymol. 339 (2001) 204–238.
[5] J.W. Peng, G. Wagner, Investigation of protein motions via relaxation measurements, Method. Enzymol. 239 (1994) 563–596.
[6] G. Wagner, NMR relaxation and protein mobility, Curr. Opin. Struc. Biol. 3 (1993) 748–754.
[7] M. Caffrey, J. Kaufman, S.J. Stahl, P.T. Wingfield, A.M. Gronenborn, G.M. Clore, 3D NMR experiments for measuring N-15 relaxation data of large proteins: Application to the 44 kDa ectodomain of SIV gp41, J. Magn. Reson. 135 (1998) 368–372.
[8] J.H. Chill, J.M. Louis, J.L. Baber, A. Bax, Measurement of N-15 relaxation in the detergent-solubilized tetrameric KcsA potassium channel, J. Biomol. NMR 36 (2006) 123–136.
[9] G. Bodenhausen, R.R. Ernst, The Accordion experiment, a simple approach to 3-dimensional NMR-spectroscopy, J. Magn. Reson. 45 (1981) 367–373.
[10] G. Bodenhausen, R.R. Ernst, Direct determination of rate constants of slow dynamic processes by two-dimensional Accordion spectroscopy in nuclear magnetic-resonance, J. Am. Chem. Soc. 104 (1982) 1304–1309.
[11] L.E. Kay, J.H. Prestegard, Spin-lattice relaxation rates of coupled spins from 2d Accordion spectroscopy, J. Magn. Reson. 77 (1988) 599–605.
[12] P.A. Carr, D.A. Fearing, A.G. Palmer, 3D accordion spectroscopy for measuring N-15 and (CO)-C-13 relaxation rates in poorly resolved NMR spectra, J. Magn. Reson. 132 (1998) 25–33.
[13] A.M. Mandel, A.G. Palmer, Measurement of relaxation-rate constants using constant-time accordion NMR-Spectroscopy, J. Magn. Reson. A 110 (1994) 62–72.
[14] H. Barkhuijsen, R. Debeer, D. Vanormondt, Improved algorithm for noniterative time-domain model-fitting to exponentially damped magnetic-resonance signals, J. Magn. Reson. 73 (1987) 553–557.
[15] Y.J. Sun, J. Rose, B.C. Wang, C.D. Hsiao, The structure of glutamine-binding protein complexed with glutamine at 1.94 angstrom resolution: comparisons with other amino acid binding proteins, J. Mol. Biol. 278 (1998) 219–229.
[16] D.R. Muhandiram, L.E. Kay, Gradient-enhanced triple-resonance 3-dimensional NMR experiments with improved sensitivity, J. Magn. Reson. B 103 (1994) 203–216.
[17] G. Barbato, M. Ikura, L.E. Kay, R.W. Pastor, A. Bax, Backbone dynamics of calmodulin studied by N-15 relaxation using inverse detected 2-dimensional NMR-spectroscopy—the central helix is flexible, Biochemistry 31 (1992) 5269–5278.
[18] F. Delaglio, S. Grzesiek, G.W. Vuister, G. Zhu, J. Pfeifer, A. Bax, NMRpipe—a multidimensional spectral processing system based on unix pipes, J. Biomol. NMR 6 (1995) 277–293.
[19] A.C. Wang, S. Grzesiek, R. Tschudin, P.J. Lodi, A. Bax, Sequential backbone assignment of isotopically enriched proteins in D2O by deuterium-decoupled Ha(Ca)N and Ha(CaCO)N, J. Biomol. NMR 5 (1995) 376–382.
[20] N. Tjandra, S.E. Feller, R.W. Pastor, A. Bax, Rotational diffusion anisotropy of human ubiquitin from N-15 NMR relaxation, J. Am. Chem. Soc. 117 (1995) 12562–12566.
[21] J.H. Yu, V. Simplaceanu, N.L. Tjandra, P.F. Cottam, J.A. Lukin, C. Ho, H-1, C-13, and N-15 NMR backbone assignments and chemical-shift-derived secondary structure of glutamine-binding protein of *Escherichia coli*, J. Biomol. NMR 9 (1997) 167–180.
[22] J.A. Jones, Optimal sampling strategies for the measurement of relaxation times in proteins, J. Magn. Reson. 126 (1997) 283–286.
[23] J. Boyd, N. Soffe, B. John, D. Plant, R. Hurd, The Generation of phase-sensitive 2d N-15-H-1 spectra using gradient pulses for coherence-transfer-pathway selection, J. Magn. Reson. 98 (1992) 660–664.
[24] A.L. Davis, J. Keeler, E.D. Laue, D. Moskau, Experiments for recording pure-absorption heteronuclear correlation spectra using pulsed field gradients, J. Magn. Reson. 98 (1992) 207–216.
[25] J.R. Tolman, J. Chung, J.H. Prestegard, Pure-phase heteronuclear multiple-quantum spectroscopy using field gradient selection, J. Magn. Reson. 98 (1992) 462–467.
[26] D. Marion, M. Ikura, R. Tschudin, A. Bax, Rapid recording of 2D NMR-spectra without phase cycling—application to the study of hydrogen-exchange in proteins, J. Magn. Reson. 85 (1989) 393–399.